PAPER • OPEN ACCESS

Design of high-quality reflectors for vertical III–V nanowire lasers on Si

To cite this article: Xin Zhang *et al* 2022 *Nanotechnology* **33** 035202

View the article online for updates and enhancements.

Design of high-quality reflectors for vertical III–V nanowire lasers on Si

Xin Zhang[1,3,5] , Hui Yang[2,5], Yunyan Zhang[1,4] and Huiyun Liu[1]

[1] Department of Electronic and Electrical Engineering, University College London, London WC1E 7JE, United Kingdom
[2] Department of Materials, Imperial College London, Exhibition Road, London SW7 2AZ, United Kingdom
[3] Faculty of Electrical Engineering and Computer Science, Ningbo University, Ningbo 315211, People's Republic of China
[4] Department of Physics, Universität Paderborn, Warburger Straße 100, D-33098, Paderborn, Germany

E-mail: yunyan.zhang@uni-paderborn.de

CrossMark

Abstract

Nanowires (NWs) with a unique one-dimensional structure can monolithically integrate high-quality III–V semiconductors onto Si platform, which is highly promising to build lasers for Si photonics. However, the lasing from vertically-standing NWs on silicon is much more difficult to achieve compared with NWs broken off from substrates, causing significant challenges in the integration. Here, the challenge of achieving vertically-standing NW lasers is systematically analysed with III–V materials, e.g. GaAs(P) and InAs(P). The poor optical reflectivity at the NW/Si interface results severe optical field leakage to the substrate, and the commonly used SiO_2 or Si_2N_3 dielectric mask at the interface can only improve it to $\sim$10%, which is the major obstacle for achieving low-threshold lasing. A NW super lattice distributed Bragg reflector is therefore proposed, which is able to greatly improve the reflectivity to >97%. This study provides a highly-feasible method to greatly improve the performance of vertically-standing NW lasers, which can boost the rapid development of Si photonics.

Keywords: nanowire, laser, vertically standing, optical leakage, super lattice distributed Bragg reflector

(Some figures may appear in colour only in the online journal)

1. Introduction

Semiconductor nanowires (NWs) lasers have a strong optical mode confinement in a very small volume, allowing lasing with diameters of a few hundred nanometers and length of a few microns [1–4]. Their small-size, low-power features endow them a wide range of novel applications [5], including Si photonics that with a big market [6]. Si photonics using optical signals offers huge advantages in speed and consumption-energy saving compared with currently-used copper-wire technology using electrical signals [7, 8]. However, Si has an indirect band gap and hence low light emitting efficiency. The lack of high-quality low-cost lasers as the signal sources on Si chips is the bottleneck of this technology. III–V materials have a direct-bandgap and therefore good optical properties, which are ideal for making high-efficiency lasers. However, when growing III–V thin-film components onto silicon, it is difficult to balance crystal quality, uniformity and area of selective growth, due to the large lattice, thermal properties, and atomic polarity differences [9–11]. When in the form of NWs, high-quality III–V materials can be monolithically grown on a Si platform [12–14]. This enables the fabrication of high-quality photonics light sources for low-cost, ultra-high
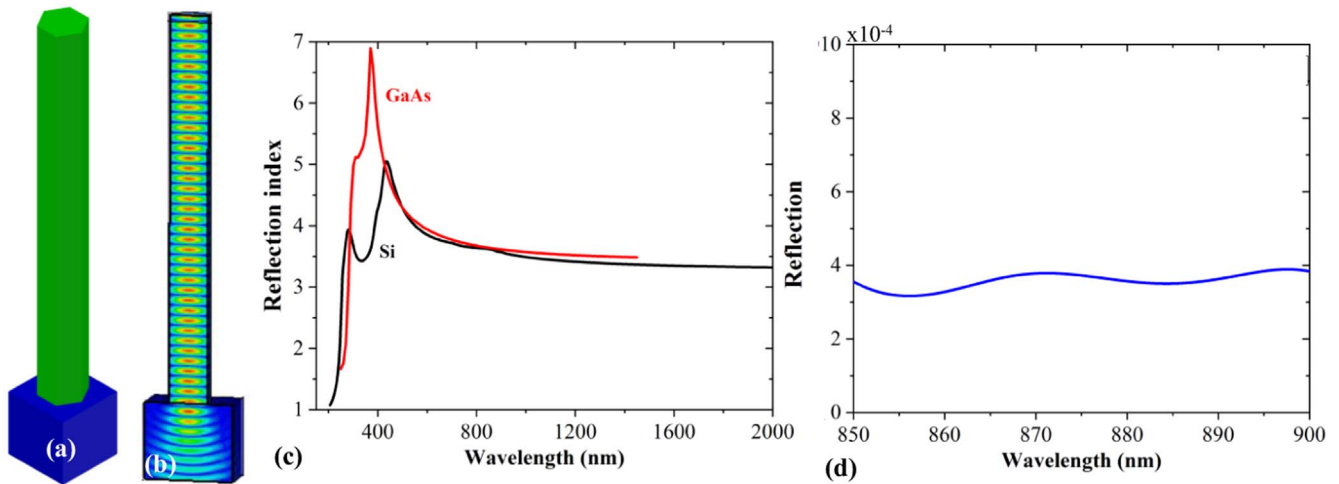
Figure 1. The light propagation and transmission behavior of a GaAs NW standing directly on Si without any special interface structure to enhance the light reflection. (a) Illustration of the structure. (b) Light-field distribution at 870 nm of (a). (c) Wavelength-dependent refraction-index difference between GaAs and Si. (d) Wavelength-dependent reflection at the NW/Si interface.

density integration on Si, solving one of the major challenges that have been limiting the Si photonics [15–19].

Whilst optically-pumped NW lasers have been widely demonstrated [20–24], majority of them were broken off from their original substrate and transferred to holder substrates. In this structure, both of the NW end facets are exposed to air with a low refractive-index ($n = {\sim}1$). The large refractive-index difference at the interface is beneficial for reflecting light back into the resonant cavity and form inverted carrier distribution. Despite the simplicity of achieving lasing with horizontal structure, NW lasers in vertically-standing structure are more desirable in most occasions due to the advantages, including massive and large-area integration, accurate allocation of NW lasers on the Si chip, simplified fabrication processes, and suitable for 3D circuit design.

However, to achieve lasing with vertically-standing structure is much more challenging, and there are only few papers on optically-pumped vertically-standing NW lasers so far [25–27]. As it has been reported, the internal quantum efficiency of the vertical NW lasers is only 16.8% [26]. This can cause enormous challenges for the fabrication of electrically-pumped lasers. One possible reason could be the similar refractive-index difference between the Si substrates and III–V materials (e.g. $n_{Si}/n_{GaAs} = {\sim}3.63/{\sim}3.59$ at 870 nm) that can cause severe optical-field leakage from the NW into the substrate and greatly degrade the quality of the optical resonant cavity. Therefore, the detailed knowledge on the causes and how to further improve performance of NW lasers are urgently needed.

In traditional thin-film devices, the super lattice (SL) distributed Bragg reflectors (DBRs) are widely used to provide strong light reflection [28, 29]. To build a high-quality DBR, material combinations with a large refractive-index difference is preferred. In the traditional thin-film growth, the strict requirement of small strain between epi-layers and substrates excludes a significant material combinations that can provide large refractive-index differences [30]. NWs with

a unique one-dimensional structure and a small cross section can provide very efficient lateral and axial strain relaxation, which can offer more advantages in this structure construction and allow various material combinations that are not allowed in thin-film structures. There have been reports on defect-free heterojunctions in NWs with large lattice mismatches, e.g. InAs/InP, InAs/InSb, GaAs/GaP [31–33]. Besides, the use of III–V materials consisting two group-V elements can produce heterojunctions with atomic sharpness, which is beneficial for achieving abrupt refractive-index change [31, 34, 35]. All these advantages can be used to construct high-quality SL DBR inside NWs. Although there have been some use of SL DBR inside NWs [36–39], there is however no report is given on the topic of vertical-standing single NW lasers so far as we know.

In this work, the light propagation and transmission behavior in NWs vertically-standing on Si has been systematically studied by numerical modeling. The severe light leakage is found from NWs to the Si substrate even with the presence of SiO_2 and Si_2N_3. A SL DBRs structure is proposed, which can effectively solve this issue.

2. Experimental section

The software used here is Comsol Multiphysics based on finite elements method. Based on the radio frequency module integrated in this software, the models of NW lasers were built based on the observation from our experiments [40, 41], and the inner light transmission field inside NWs was simulated. This research started with GaAs(P) NW lasers, because majority of reports in literature are GaAs-based and the obtained knowledge can also be used to other material systems. The NW laser structure can be seen in figure 1(a). The GaAs NW is standing vertically on a Si substrate with a diameter of ${\sim}500$ nm and length of ${\sim}10\ \mu$m, acting as both the gain material and the resonant cavity. The choose of
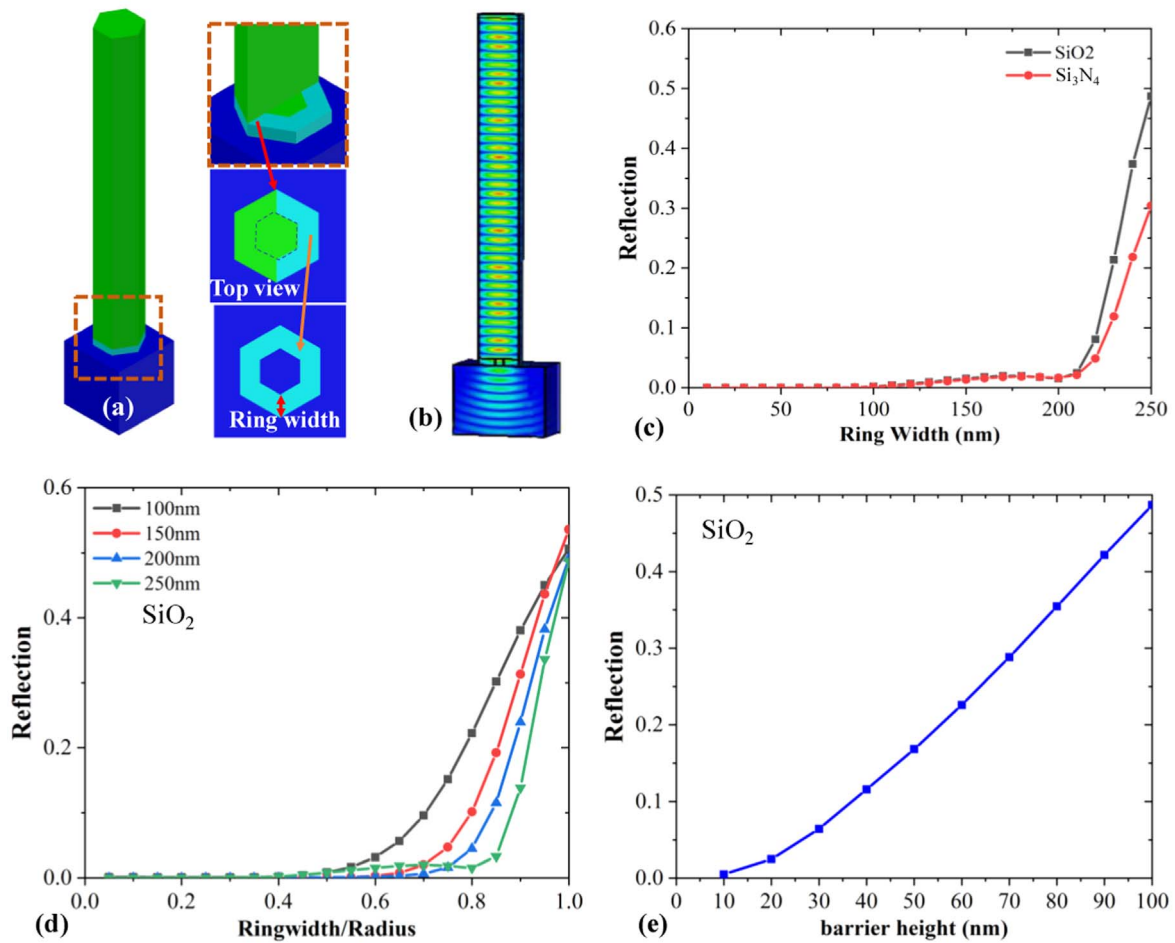
Figure 2. The light propagation and transmission behaviour of a GaAs NW (500 nm) standing directly on Si with a hexagon ring dielectric layer to enhance the light reflection. (a) Illustration of the dielectric ring reflector. (b) Light-field distribution at 870 nm of the GaAs NW with a 230 nm width 100 nm thick SiO_2 interface layer. (c) Ring-width-dependent reflection of a GaAs NW with a 100 nm thick of SiO_2 or Si_3N_4 layer. (d) Influence of SiO_2 ring width/radius ratio on the reflection of NW of different size. (e) SiO_2 Dielectric thickness-dependent reflection of a GaAs NW with a 250 nm width SiO_2 interface layer.

500 nm diameter is due to the low loss at this size [42]. The center wavelength of laser is selected to be 870 nm which is the GaAs emission wavelength at the room temperature. We assume the laser beams with the same intensity propagating from the NW to the NW/Si interface and integrate the reflection energy right above the interface.

3. Results and discussion

GaAs NWs are commonly grown directly on Si substrates without special interface structure to enhance the light reflection, which is shown in figure 1(a). As can be seen from the light-field distribution shown in figure 1(b), there is severe light energy leakage from the NW into the substrate. The refraction-index difference at the NW/Si interface is very small for the wavelength >500 nm shown in figure 1(c). As a result, the reflection at the interface is ~4×10^{-5} at the wavelength $850 - 890$ nm (figure 1(d)). This phenomenon is highly beneficial for constructing tandem photovoltaics, such as the III–V NW/Si two junction solar cells. As demonstrated by Diedenhofen *et al* [43], more than 90% of the photons,

with the energy lower than the InP absorption, were coupled into the underlying substrate by the InP NWs. However, it brings big challenges in the formation of proper resonant cavities for lasers with this configuration. Therefore, proper structure design is needed to reduce light leaking into the substrate.

Si_3N_4 ($n = \sim2.347$ at 870 nm) and SiO_2 ($n = \sim1.44$ at 870 nm) are widely used as the pattern mask to do the positioned NW growth on Si substrate [13], and they have a much lower refractive-index compared with III–Vs (e.g. $n_{GaAs} = \sim3.5$ at 870 nm). Thus, they can be potentially used to enhance the light reflection at the interface. A hexagonal ring-shaped dielectric reflector is therefore studied here (figure 2(a)). It needs to be mentioned that the inner hole is normally circular in practice due to the resolution limitation in the patterned substrate fabrication processes. The ring hole in the centre of the reflector is the opening for the NW growth with substrate lattice template. As can be seen from the light-field distribution in the NWs in figure 2(b), the optical field leakage into the substrate reduces compared with figure 1(b) when the dielectric layer with a thickness of 100 nm is introduced at the interface. Both dielectric layers with a large
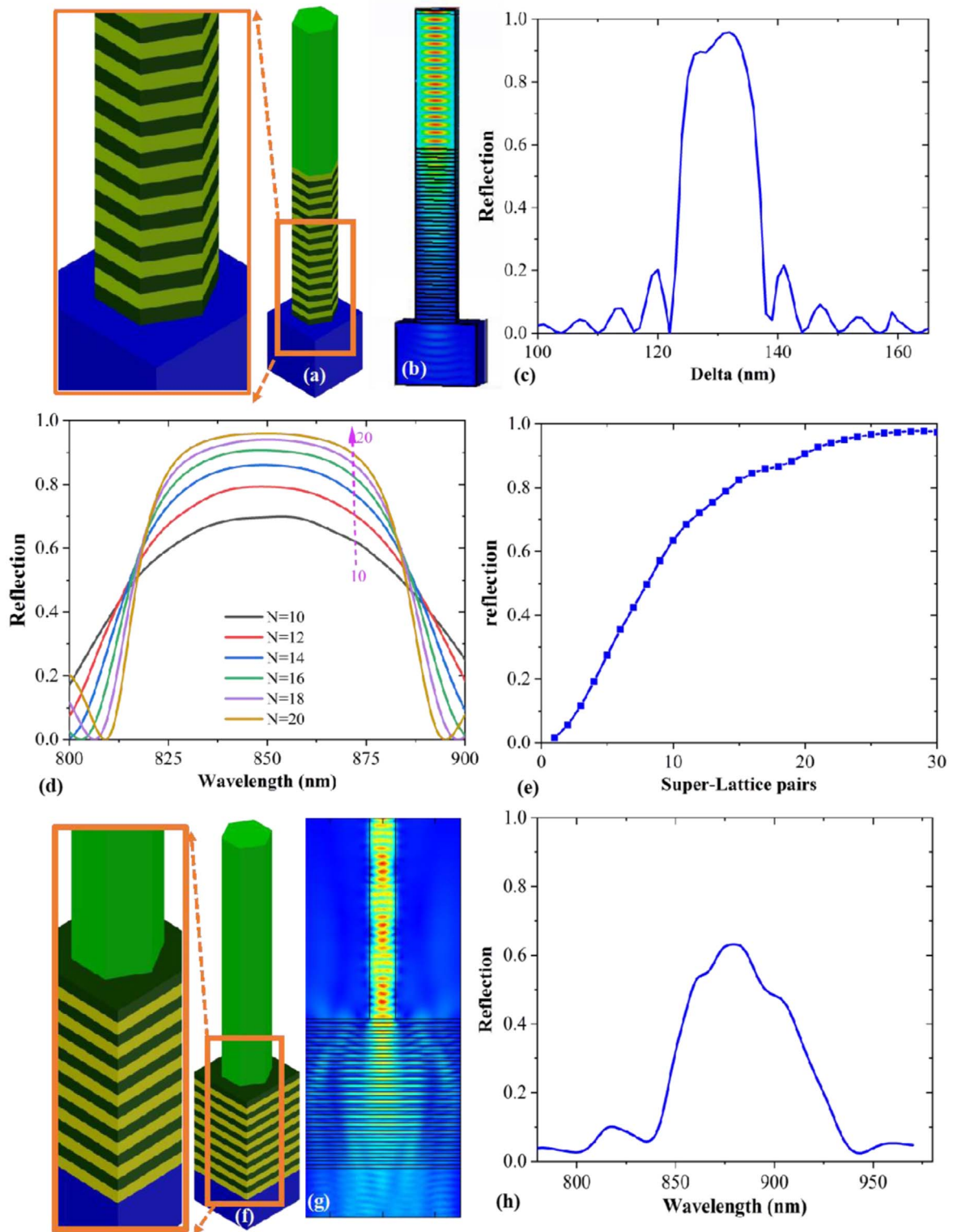
Figure 3. The light propagation and transmission behavior of a GaAs NW standing directly on Si with a SL DBR to enhance the light reflection. (a)–(e) are from the structure with a NW DBR reflector. (a) Illustration of the structure. (b) Light-field distribution at 870 nm of the NW. (c) SL-period-dependent light reflection at 870 nm. (d) Reflection spectra of DBRs with different SL pairs. (e) SL-pairs-dependent light reflection at 870 nm. (f)–(h) are from the structure with a substrate DBR reflector. (f) Illustration of the structure. (g) Light-field distribution at 870 nm of the NW. (h) Light reflection spectrum at the NW/substrate interface.
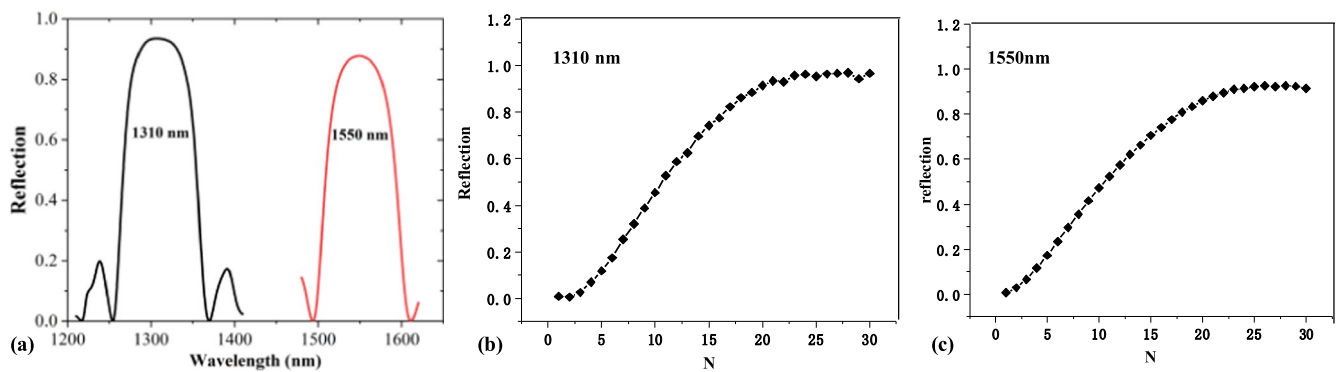
Figure 4. (a) Reflection spectra of 20-pair SL DBRs that work for 1310 and 1550 nm lasers. (b) and (c) Influence of SL pairs on the light reflection.

ring width, defined to be the thickness of concentric hexagon with the outer edge the same size as the NW, can increase the reflection to above 30%, which is shown in figure 2(c). However, the interface reflectance is small (<3%) for small ring widths and rises slowly with the increase of the width; only when the width is approaching the NW diameter, the reflectance rises rapidly. This phenomenon is the same for NWs of different diameters we study (figure 2(d)), which suggest that the width of dielectric needs to be at least over half the size of the NW to get more apparent reflection. It needs to be noted that the interface reflection of NWs with a SiO_2 layer can be up to 67% higher than that of Si_3N_4 layer at a large ring width, which is due to the larger index difference with the NW. Consequently, it would be better to choose SiO_2 as the reflector material when building lasers. Moreover, the thickness of the dielectric layer can greatly influence the reflectance. As is shown in figure 2(e), the reflection of the NWs with a SiO_2 dielectric layer grows almost linear to ∼50% at 100 nm. At present, the thickness of dielectric pattern is normally between 20 and 30 nm, which can only provide a low reflectivity of ∼10%. We have not notice the reports using thicker patterns. More study is needed about growing on super-thick patterns, such as 100 or 200 nm, which can however bring high challenges on both the pattern making and NW growth.

With the assumption that a 100 nm thick dielectric reflector between the NW/Si interface can be easily used, the reflection can only be improved to ∼50% and a high percentage of the light is still lost through the substrate, causing high threshold of electrically-pumped lasers. Considering the advantages of NWs in the construction of heterojunctions by switching group-V elements as mentioned above, a $GaAs_{0.1}P_{0.9}/GaAs$ ($n_{GaAsP}/n_{GaAs} = 3.2/3.59$) SL DBR can be introduced between NW and Si substrate (figure 3(a)). As can be seen from the light-field distribution in figure 3(b), most of light-field is resonating inside the NW with only little light energy leaks into the substrate. The SL period is one of the key parameters that decide the peak reflection wavelength. For a lasing wavelength of 870 nm, a high reflectance of over 80% can be achieved with a period between 124 and 142 nm, and the reflection reaches the maximum can be 96% at 136 nm (figure 3(c)). The pair of SL

can also significantly influence the light reflection. As can be seem in figure 3(d), the reflection increases rapidly with the increase of the SL pairs to 15 and gradually saturates after 20 pairs. The reflection at 870 nm can reach 0.96 with a 20-pair SL and 0.98 with a 30-pair SL. It needs to be mentioned that the SL DBR can have a large reflection window. For example, its reflectance can maintain above 90% between 820 and 880 nm. Thus, the SL DBR has significant advantages over the dielectric reflectors.

The technique is well developed for growing the SL DBR on substrate surface in the form of thin-film structure. Integrating NWs directly onto the substrates with DBRs (figure 3(f)) can provide a possibility to avoid the complexity of growing DBR into NWs, which has been widely used experimentally [44–46]. Thus, the influence of the location on the reflection effect of SL DBR is also studied with the optimized DBR parameters used in figure 3(c). It needs to be mentioned that we only intend to make a direct comparison of the two structures, and assume that the lattice mis-match in the substrate DBR growth is not an issue. As can be seen from figure 3(g), the DBR can effectively avoid the leakage of the optical field into the substrate. However, the field disperses after coming out of the NW bottom into the substrates, and a significant portion of the energy can no longer be reflected back to the NWs with a small cross section. As supported by the reflection spectrum in figure 3(h), the energy in the NW at the peak wavelength can only maintain at ∼60%, which is greatly reduced compared with that of the NW DBR.

The studied method is also extended to telecom communication wavelength. The NWs used here are made of InAsP. The InAs/InP lattice periods are 0.236 μm for 1310 nm light and 0.28 μm for 1550 nm light respectively. As can be seen in figure 4, the SL DBR can also work well with these lasers and both of them can improve the light reflection to above 90% when the SL pairs are over 20.

So far as we know, there is still lack of experiment report on the vertically-standing single nanowire lasers with this design. More experiment effort is needed. Besides, Heo *et al* [38] reported the building of quasi-film DBR reflector in the high density nanowire arrays, and increased the light reflection to above 70%. This can partially support the feasibility of using our design in the vertically-standing single NW lasers.

4. Conclusions

In summary, the challenge of achieving vertically-standing NW lasers on Si is systematically analyzed. The optical reflectivity at the GaAs NW/Si interface is $\sim 4 \times 10^{-5}$ at the wavelength 850– 890 nm, which is due to the small refraction-index difference between GaAs and Si. This small reflectivity prevents the formation of acceptable optical resonant cavity for the realization of lasing. SiO_2 and Si_2N_3, with larger refraction-index differences with Si, are widely used in the NW growth, which is however can only improve it to $\sim 10\%$ and majority of the energy is still leaking into the substrates. To further improve the reflectivity at NW/substrate interfaces, the NW SL DBR is proposed, which can greatly improve the reflectance to 97%, allowing the formation of high-quality optical resonant cavity. Besides, these reflectors can also be used for telecom communication wavelength (1310 nm and 1550 nm) and a high reflectance of $\sim 90\%$ can be achieved. It needs to be mentioned that the SL growth in NWs will need a large change in growth fluxes and hence the growth environment, which can lead to the generation of stacking faults. A carefully balanced growth environment will be needed in the DBR growth [47]. This research provides useful information for the design of high-quality vertically-standing NW lasers onto Si platform, which can be widely used in the integrated circuits.

Acknowledgments

Data availability statement

All data that support the findings of this study are included within the article (and any supplementary files).

Notes

The authors declare no competing financial interest.

ORCID iDs

Xin Zhang ⬤ https://orcid.org/0000-0002-6669-7037
Yunyan Zhang ⬤ https://orcid.org/0000-0002-2196-7291
Huiyun Liu ⬤ https://orcid.org/0000-0002-7654-8553

References

[1] Cui Y, Wei Q Q, Park H K and Lieber C M 2001 Nanowire nanosensors for highly sensitive and selective detection of biological and chemical species *Science* **293** 1289–92

[2] Horth A and Quitoriano N J 2012 Novel, low-index waveguide as laser external cavity *Opt. Express* **20** 11137–42

[3] Wang J, Gudiksen M S, Duan X, Cui Y and Lieber C M 2001 Highly polarized photoluminescence and photodetection from single indium phosphide nanowires *Science* **293** 1455–7

[4] Yan R, Gargas D and Yang P 2009 Nanowire photonics *Nat. Photon.* **3** 569–76

[5] Zhang Y, Wu J, Aagesen M and Liu H 2015 III–V nanowires and nanowire optoelectronic devices *J. Phys. D: Appl. Phys.* **48** 463001

[6] Paul D J 2009 Silicon photonics: a bright future? *Electron. Lett.* **45** 582–4

[7] Liu M, Zhang M, Zhao W, Song C, Wang D, Li Q and Wang Z 2017 Prediction of congestion degree for optical networks based on bp artificial neural network *2017 16th Int. Conf. on Optical Communications and Networks (ICOCN)* (Piscataway, NJ: IEEE) pp 1–3

[8] J Ni J and Bai X 2017 A review of air conditioning energy performance in data centers *Renew. Sustain. Energy Rev.* **67** 625–40

[9] Fitzgerald E A and Chand N 1991 Epitaxial necking in GaAs grown on pre-pattemed Si substrates *J. Electron. Mater.* **20** 839–53

[10] Chang J S, Carey K W, Turner J E and Hodge L A 1990 Compositional non-uniformities in selective area growth of GaInAs on InP grown by OMVPE *J. Electron. Mater.* **19** 345–8

[11] Wang Z, Abbasi A, Dave U, De Groote A, Kumari S, Kunert B and Roelkens G 2017 Novel light source integration approaches for silicon photonics *Laser Photon. Rev.* **11** 1700063

[12] Li K H, Liu X, Wang Q, Zhao S and Mi Z 2015 Ultralow-threshold electrically injected AlGaN nanowire ultraviolet lasers on Si operating at low temperature *Nat. Nanotechnol.* **10** 140–4

[13] Zhang Y, Wu J, Aagesen M, Holm J, Hatch S, Tang M, Huo S and Liu H 2014 Self-catalyzed ternary core–shell GaAsP nanowire arrays grown on patterned Si substrates by molecular beam epitaxy *Nano Lett.* **14** 4542–7

[14] Frost T, Jahangir S, Stark E, Deshpande S, Hazari A, Zhao C, Ooi B S and Bhattacharya P 2014 Monolithic electrically injected nanowire array edge-emitting laser on (001) silicon *Nano Lett.* **14** 4535–41

[15] Saxena D, Mokkapati S, Parkinson P, Jiang N, Gao Q, Tan H H and Jagadish C 2013 Optically pumped room-temperature GaAs nanowire lasers *Nat. Photon.* **7** 963–88

[16] Fischer R, Masselink W T, Klem J, Henderson T, McGlinn T C, Klein M V, Morkoç H, Mazur J H and Washburn J 1985 Growth and properties of GaAs/AlGaAs on nonpolar substrates using molecular beam epitaxy *J. Appl. Phys.* **58** 374–81

[17] Kim H, Lee W J, Farrell A C, Morales J S, Senanayake P, Prikhodko S V, Ochalski T J and Huffaker D L 2017 Monolithic InGaAs nanowire array lasers on silicon-on-insulator operating at room temperature *Nano Lett.* **17** 3465–70

[18] Liang D and Bowers J E 2010 Recent progress in lasers on silicon *Nat. Photon.* **4** 511–7

[19] Won R and Mario P 2010 Integrating silicon photonics *Nat. Photon.* **4** 498–9

[20] Guilhabert B, Hurtado A, Jevtics D, Gao Q, Tan H H, Jagadish C and Dawson M D 2016 Transfer printing of semiconductor nanowires with lasing emission for controllable nanophotonic device fabrication *ACS Nano* **10** 3951–8

[21] Zhang Y, Saxena D, Aagesen M and Liu H 2019 Toward electrically driven semiconductor nanowire lasers *Nanotechnology* **30** 192002

[22] Xu W Z *et al* 2018 Vertically emitting indium phosphide nanowire lasers *Nano Lett.* **18** 3414–20

[23] Stettner T *et al* 2016 Coaxial GaAs-AlGaAs core-multishell nanowire lasers with epitaxial gain control *Appl. Phys. Lett.* **108** 011108

[24] Tatebayashi J, Kako S, Ho J, Ota Y, Iwamoto S and Arakawa Y 2015 Room-temperature lasing in a single nanowire with quantum dots *Nat. Photon.* **9** 501–5

[25] Mayer B, Janker L, Loitsch B, Treu J, Kostenbader T, Lichtmannecker S and Gies C 2015 Monolithically integrated high-β nanowire lasers on silicon *Nano Lett.* **16** 152–6

[26] Sun H, Ren F, Ng K W, Tran T T D, Li K and Chang-Hasnain C J 2014 Nanopillar lasers directly grown on silicon with heterostructure surface passivation *Acs Nano* **8** 6833–9

[27] Chen R, Tran T T D, Ng K W, Ko W S, Chuang L C, Sedgwick F G and Chang-Hasnain C 2011 Nanolasers grown on silicon *Nat. Photon.* **5** 170–5

[28] Mastro M A, Holm R T, Bassim N D, Eddy C R Jr, Gaskill D K, Henry R L and Twigg M E 2005 High-reflectance III-nitride distributed Bragg reflectors grown on Si substrates *Appl. Phys. Lett.* **87** 241103

[29] Huang G S, Lu T C, Yao H H, Kuo H C, Wang S C, Lin C W and Chang L 2006 Crack-free distributed Bragg reflectors incorporated with superlattices grown by metalorganic chemical vapor deposition *Appl. Phys. Lett.* **88** 061904

[30] Shi J Y, Yu L P, Wang Y Z, Zhang G Y and Zhang H 2002 Influence of different types of threading dislocations on the carrier mobility and photoluminescence in epitaxial GaN *Appl. Phys. Lett.* **80** 2293–5

[31] Larsson M W, Wagner J B, Wallin M, Håkansson P, Fröberg L E, Samuelson L and Wallenberg L R 2006 Strain mapping in free-standing heterostructured wurtzite InAs/InP nanowires *Nanotechnology* **18** 015504

[32] Ercolani D, Rossi F, Li A, Roddaro S, Grillo V, Salviati G, Beltram F and Sorba L 2009 InAs/InSb nanowire heterostructures grown by chemical beam epitaxy *Nanotechnology* **20** 505605

[33] Zhang G, Tateno K, Gotoh H, Sogawa T and Nakano H 2010 Structural compositional and optical characterizations of vertically aligned AlAs/GaAs/GaP heterostructure nanowires epitaxially grown on Si substrate *Jpn. J. Appl. Phys.* **49** 015001

[34] Priante G, Patriarche G, Oehler F, Glas F and Harmand J C 2015 Abrupt GaP/GaAs interfaces in self-catalyzed nanowires *Nano Lett.* **15** 6036–41

[35] Zhang Y *et al* 2020 Defect-free axial GaAs/GaAsP nanowire quantum dots with strong carrier confinement *Nano Lett.* **21** 5722

[36] Fu A, Gao H, Petrov P and Yang P 2015 Widely tunable distributed Bragg reflectors integrated into nanowire waveguides *Nano Lett.* **15** 6909–13

[37] Aghaeipour M and Pettersson H 2018 Enhanced broadband absorption in nanowire arrays with integrated Bragg reflectors *Nanophotonics* **7** 819–25

[38] Heo J, Zhou Z, Guo W, Ooi B S and Bhattacharya P 2013 Characteristics of AlN/GaN nanowire Bragg mirror grown on (001) silicon by molecular beam epitaxy *Appl. Phys. Lett.* **103** 181102

[39] Svendsen G K, Weman H and Skaar J 2012 Investigations of Bragg reflectors in nanowire lasers *J. Appl. Phys.* **111** 123102

[40] Wu J *et al* 2016 Defect-free self-catalyzed GaAs/GaAsP nanowire quantum dots grown on silicon substrate *Nano Lett.* **16** 504–11

[41] Zhang Y and Liu H 2020 Self-catalyzed GaAs (P) nanowires and their application for solar cells *J. Phys. D: Appl. Phys.* **53** 233001

[42] Saxena D, Jiang N, Yuan X, Mokkapati S, Guo Y, Tan H H and Jagadish C 2016 Design and room-temperature operation of GaAs/AlGaAs multiple quantum well nanowire lasers *Nano Lett.* **16** 5080–6

[43] Diedenhofen S L, Janssen O T, Grzela G, Bakkers E P and Gómez Rivas J 2011 Strong geometrical dependence of the absorption of light in arrays of semiconductor nanowires *ACS Nano* **5** 2316–23

[44] Tatebayashi J, Kako S, Ho J, Ota Y, Iwamoto S and Arakawa Y 2017 Growth of InGaAs/GaAs nanowire-quantum dots on AlGaAs/GaAs distributed Bragg reflectors for laser applications *J. Cryst. Growth* **468** 144–8

[45] Bashar S B, Suja M, Shi W and Liu J 2016 Enhanced random lasing from distributed Bragg reflector assisted Au–ZnO nanowire schottky diode *Appl. Phys. Lett.* **109** 192101

[46] Huang J, Monzur Morshed M, Zuo Z and Liu J 2014 Distributed Bragg reflector assisted low-threshold ZnO nanowire random laser diode *Appl. Phys. Lett.* **104** 131107

[47] Zhang Y, Velichko A V, Fonseka H A, Parkinson P, Davis G, Gott J A, Aagesen M, Sanchez A M, Mowbray D and Liu H 2021 Defect-free axially-stacked GaAs/GaAsP Nanowire quantum dots with strong carrier confinement *Nano Lett.* **21** 5722–9